Research Square

Preprints are preliminary reports that have not undergone peer review.
They should not be considered conclusive, used to inform clinical practice,
or referenced by the media as validated information.

DNA methylation profiling classifies lateral ventricular neurocytomas with lipidized cells as central neurocytoma

Takeru Kuwabara
Hokkaido University
Yoshitaka Oda
Hokkaido University
Zen-ichi Tanei
Hokkaido University Hospital
Satoshi Tanikawa
Hokkaido University
Yui Moritsugu
Hokkaido University Hospital
Tomohito Yamauchi
Hokkaido University
Koki Ise
Hokkaido University
Yusuke Shirai
Hokkaido University
Marie Katou
Hokkaido University
Hirokazu Sugino
Hokkaido University Hospital
Lei Wang
Hokkaido University
Yusuke Fujiwara
Sapporo Shuyukai Hospital, Medical Corporation Shuyukai
Hiroaki Motegi
Sapporo Azabu Neurosurgical Hospital
Yukitomo Ishi
Hokkaido University
Shigeru Yamaguchi
Hokkaido University
Masumi Tsuda

Hokkaido University
Kaishi Satomi
Kyorin University
Junji Shibahara
Kyorin University
Miki Fujimura
Hokkaido University
Shinya Tanaka
tanaka@med.hokudai.ac.jp

Hokkaido University

Research Article

Keywords: Central neurocytoma, Liponeurocytoma, Lipidized cells, DNA methylation, Perilipin-1

Posted Date: November 25th, 2026

DOI: https://doi.org/10.21203/rs.3.rs-11674555/v1

License: This work is licensed under a Creative Commons Attribution 4.0 International License.
Read Full License

Additional Declarations: No competing interests reported.

Original Article

DNA methylation profiling classifies lateral ventricular neurocytomas with lipidized cells as central neurocytoma

Takeru Kuwabara[1], Yoshitaka Oda[1], Zen-ichi Tanei[2], Satoshi Tanikawa[1], Yui Moritsugu[2], Tomohito Yamauchi[3], Koki Ise[1,2], Yusuke Shirai[1,4], Marie Katou[1], Hirokazu Sugino[2], Lei Wang[1,5], Yusuke Fujiwara[6], Hiroaki Motegi[7], Yukitomo Ishi[8], Shigeru Yamaguchi[8], Masumi Tsuda[1,4,5], Kaishi Satomi[9], Junji Shibahara[9], Miki Fujimura[8], Shinya Tanaka[1,2,4,5]

[1]Department of Cancer Pathology, Faculty of Medicine, Hokkaido University, Sapporo, Japan

[2]Department of Surgical Pathology, Hokkaido University Hospital, Sapporo, Japan

[3]Department of Medicine, School of Medicine, Hokkaido University, Sapporo, Japan

[4]Institute for Chemical Reaction Design and Discovery (WPI-ICReDD), Hokkaido University, Sapporo, Japan

[5]Division of Next-Generation Pathology Innovation, Faculty of Medicine, Hokkaido University, Sapporo, Japan

[6]Department of Neurosurgery, Sapporo Shuyukai Hospital, Medical Corporation Shuyukai, Sapporo, Japan

[7]Department of Neurosurgery, Sapporo Azabu Neurosurgical Hospital, Sapporo, Japan

[8]Department of Neurosurgery, Faculty of Medicine, Hokkaido University, Sapporo, Japan

[9]Department of Pathology, Kyorin University School of Medicine, Mitaka, Japan

Corresponding author: Shinya Tanaka, Department of Cancer Pathology, Faculty of Medicine, Hokkaido University, Kita 15, Nishi 7, Kita-ku, Sapporo 060-8638, Japan. Tel:

23 +81-11-706-7806, Fax: +81-11-706-5902, E-mail: tanaka@med.hokudai.ac.jp

24 Word count: 6,392

Abstract

Neurocytomas are classified into central neurocytoma (CN), extraventricular neurocytoma, and cerebellar liponeurocytoma (LIPN). Each of these forms a distinct DNA methylation class. Lipidized cells, the hallmark of LIPN, also occur in lateral ventricular neurocytomas, but whether these tumors belong to CN or LIPN, or represent a distinct entity, is unresolved. We analyzed three lateral ventricular neurocytomas with lipidized cells by immunohistochemistry and DNA methylation profiling. In all cases, perilipin-1 outlined the large lipid droplets of lipidized cells and labeled small droplets in tumor cells. All three cases were classified as CN by the Heidelberg classifier and two crossNN models. In unsupervised analysis with public reference data, they clustered with reference CN, and not with LIPN or sellar region neurocytoma (SELN). A crossNN model retrained with SELN recognized SELN in cross-validation but nonetheless classified the cases as CN. Copy-number profiles were flat, without the chromosome 14 and 2p losses seen in LIPN, and the cases showed CN-like global and *FGFR3* hypomethylation. These findings support the classification of lateral ventricular neurocytomas with lipidized cells as CN. Lipidized cells are therefore not specific to LIPN and may arise from lipid accumulation in tumor cells.

Keywords Central neurocytoma · Liponeurocytoma · Lipidized cells · DNA methylation · Perilipin-1

Introduction

Neurocytomas are neuronal tumors composed of uniform round cells with fibrillary areas [29]. The WHO classification distinguishes central neurocytoma (CN), extraventricular neurocytoma (EVN), and cerebellar liponeurocytoma (LIPN), largely by location [29]. CN arises in the lateral and third ventricles of young adults [29]. EVN arises outside the ventricular system and frequently harbors *FGFR1–TACC1* fusion [26, 29]. LIPN arises in the cerebellum of adults and is characterized by lipidized cells resembling mature adipocytes [10, 29].

DNA methylation profiling has become an essential tool for defining central nervous system tumor entities [6, 29]. CN and LIPN form distinct DNA methylation classes [6, 7]. Initially, EVN did not consistently match any existing class [7], but was later found to form a distinct class [17, 26, 27]. CN shows global and *FGFR3* hypomethylation [15, 16], and most CN have flat copy-number profiles [29], whereas LIPN frequently show losses of chromosome 14 and 2p [6]. About half of methylation-defined EVN show copy-number changes indicating *FGFR1–TACC1* or *FGFR3–TACC3* fusion [26]. Sellar region neurocytoma (SELN), which shows a CpG island methylator phenotype, was recently shown to form a separate methylation group that is not yet represented in current classifiers [20]. The same study reported methylation changes at adipogenesis-related genes, such as *ZFPM1* and *NFATC1*, in LIPN [20].

Although lipidized cells are characteristic of LIPN, they also occur in lateral ventricular neurocytomas, which have been reported under various names [1, 11, 13, 30]. The term central liponeurocytoma has been proposed to encompass these tumors and LIPN [30]. Lipidized cells have been attributed to lipid accumulation in tumor cells or to differentiation of tumor cells into adipocyte-like cells [2, 11]. Whether lateral ventricular neurocytomas with lipidized cells belong to CN, LIPN, or another group such as SELN, or form a distinct

methylation class, has not been determined.

In this study, we analyzed three lateral ventricular neurocytomas containing lipidized cells by immunohistochemistry and DNA methylation profiling, and compared them with public data of neurocytomas, other brain tumors, and non-neoplastic brain tissue.

Materials and methods

Patients and samples

Three lateral ventricular neurocytomas containing lipidized cells were diagnosed at the Department of Cancer Pathology, Faculty of Medicine, Hokkaido University (Cases 1 and 3) and at Hokkaido University Hospital (Case 2) between 2024 and 2025. Formalin-fixed, paraffin-embedded (FFPE) tumor tissue was available for all cases, and clinical information was obtained from the medical records.

Histology and immunohistochemistry

Sections were stained with hematoxylin and eosin and immunohistochemically with antibodies against synaptophysin, NeuN, GFAP, OLIG2, Ki-67 (MIB-1), and perilipin-1 (Online Resource 1). The MIB-1 labeling index was calculated with QuPath (v0.7.0) [4] as the percentage of positive nuclei within a hot-spot area annotated on each whole-slide image, with identical settings for all cases (Online Resource 1). Immunoreactivity was assessed separately in tumor cells and in lipidized cells, which were identified by a unilocular droplet and a peripherally displaced nucleus. All assessments other than the MIB-1 labeling index were qualitative.

DNA methylation array

DNA was extracted from FFPE tissue and analyzed on the Infinium MethylationEPIC v2.0 BeadChip (EPICv2, Illumina, San Diego, CA, USA) at the Department of Pathology, Kyorin University School of Medicine. Data were analyzed in R (v4.6.0) with Bioconductor (v3.23)

and in Python (v3.12.2) with PyTorch (v2.14.0). Claude (Anthropic) was used to assist with writing the manuscript and the analysis code.

Supervised classification

IDAT files were uploaded to the Heidelberg CNS Tumor Methylation Classifier v12.8 (Epignostix, https://app.epignostix.com) [6, 27], in which a calibrated score ≥ 0.9 is regarded as a match. Classification was also performed with two published crossNN models [31], one trained on the Heidelberg reference cohort (91 classes) [6] and the other a pan-cancer model (178 classes). For crossNN, IDAT files were processed individually with minfi (v1.58.0) [3], and confidence scores > 0.4 were regarded as valid [31]. Arrays were required to meet the quality criteria of the Heidelberg reference data [27]. For replicate probes on the EPICv2 array, one probe per locus was selected according to the hierarchy of Pearce et al. [20, 22]. As controls, 90 primary CN from GSE288337 profiled on the MethylationEPIC (EPIC) array (after removal of seven duplicate profiles, Online Resource 1) [15], 21 CN and 10 LIPN of the Heidelberg reference cohort (GSE90496, HumanMethylation450 [450K] array) [6], and two EVN from GSE152653 [17] were processed identically. Because the Heidelberg-cohort model has no EVN class, an EVN was regarded as correctly handled when it was not classified as CN [7]. Because neither model contains a SELN class, the Heidelberg-cohort model was retrained with the 20 SELN in GSE331022 [20] added as a 92nd class and evaluated by fivefold cross-validation [31]. A final model trained with all 20 SELN was then applied to the cases and controls. Details are given in Online Resource 1.

Unsupervised analysis

IDAT files of the cases and reference samples were processed individually with SeSAMe (v1.30.1) [33] following the pipeline of Pearce et al. [20]. The reference set comprised the 90 CN from GSE288337 [15], the two EVN from GSE152653 [17], the 20 SELN from GSE331022 [20], and the 21 CN and 10 LIPN from GSE90496 [6]. Samples of the main

differential diagnoses of CN (seven classes, 169 samples) and non-neoplastic brain (30 samples) were also included from GSE90496, up to 30 per class [6]. Probes shared by all platforms without missing values, excluding those on the sex chromosomes, were used. Array type was not corrected because it was largely confounded with sample group. As in the Heidelberg classifier v12.8 [27], the 10,000 most variable probes were embedded with uniform manifold approximation and projection (UMAP) [19] using uwot (v0.2.5) with default parameters. The embedding was repeated with n_neighbors = 5, 20, and 80 [19] and after correction for FFPE versus frozen material. Similarity was assessed by Pearson correlation on the 32,000 most variable probes, as in the analysis of the Heidelberg reference cohort [6].

Copy-number analysis

Copy-number profiles of the cases and of the ten LIPN, 90 CN, and 20 SELN in the reference set were generated with conumee2 (v2.1.2) [8]. Thirty non-neoplastic brain samples in the reference set served as the normal reference [8]. Samples with a noise parameter > 0.6 were excluded [8]. Arm-level log2 ratios were calculated as probe-weighted means of segment values [33], and gains and losses were called at ±0.1 [9]. To detect copy-number changes indicating *FGFR1–TACC1* or *FGFR3–TACC3* fusion [26], we calculated for each sample the mean log2 ratio of the probes between *FGFR1* and *TACC1* minus the median log2 ratio of the other probes on the same chromosome, and compared the values of the cases with those of the CN from GSE288337 and the two EVN after the same noise exclusion. The region spanning *FGFR3* and *TACC3* was assessed likewise. Profiles generated by the Heidelberg classifier were also reviewed.

Global and FGFR3 methylation

Following Eckhardt et al. [9], global methylation was defined as the mean of all beta values per sample after minfi noob preprocessing and removal of probes containing single-

nucleotide polymorphisms and of probes on the X and Y chromosomes. Reference CN and non-neoplastic brain samples were compared by Welch's t-test. *FGFR3* methylation was assessed as the mean beta value of the three CN-specific CpGs reported by Lee et al. (cg00525145, cg08145949, and cg11777917) [16].

Comparison of CN and LIPN

The 21 CN and 10 LIPN of GSE90496 [6] were compared following Pearce et al. [20]. Differentially methylated CpGs (limma [24], adjusted P value < 0.01, $|\Delta\beta| > 0.20$) and differentially methylated regions (DMRs, DMRcate [21], $|\Delta\beta| > 0.20$) were identified. DMRs were validated in GSE109379 (two CN and one LIPN) [6] and tested for gene-set enrichment [18]. A LIPN score was calculated as the mean beta value of DMRs hypermethylated in LIPN minus that of DMRs hypomethylated in LIPN. The methylation of 17 adipogenesis-related genes, including *ZFPM1* and *NFATC1* [20], was evaluated in all samples (Online Resource 1).

Results

Clinical and histological features

All three patients were men, aged 34 (Case 1), 80 (Case 2), and 34 (Case 3) years. All tumors were located in the lateral ventricle and were removed by craniotomy (Table 1).

Table 1 Clinicopathological and molecular features of the three cases

	Case 1	**Case 2**	**Case 3**
Age (years)/sex	34/M	80/M	34/M
Location	Lateral ventricle	Lateral ventricle	Lateral ventricle
Symptoms	Depressed mood, memory impairment, diplopia	Symptomatic epilepsy, abnormal sensation in the left fingers, left lower-limb weakness	Headache, orthostatic dizziness, visual field constriction in the right eye
Tumor cells: SYN / NeuN / GFAP / OLIG2	+ / + in many / − / −	+ / + in many / − / −	+ / + in many / − / −
MIB-1 labeling index, % (positive/counted nuclei)	2.1 (407/19,182)	2.1 (224/10,559)	1.9 (234/12,260)

	Case 1	Case 2	Case 3
Lipidized cells: PLIN1 / SYN around droplet	rim+ / absent in some	rim+ / absent in some	rim+ / absent in some
PLIN1+ droplets in tumor cells	Small	Small and medium-sized	Small and medium-sized
Heidelberg classifier v12.8 (score)	CN (0.998)	CN (0.990)	CN (0.999)
crossNN, Heidelberg-cohort model (score)	CN (0.72)	CN (0.76)	CN (0.77)
crossNN, pan-cancer model (score)	CN (0.57)	CN (0.65)	CN (0.64)
Copy-number profile	Flat	Flat	Flat

CN central neurocytoma, M male, PLIN1 perilipin-1, rim+ positive rim around the droplet, SYN synaptophysin

Histologically, all tumors consisted of uniform round cells with finely granular chromatin, small nucleoli, and pale eosinophilic cytoplasm, which proliferated diffusely in a fibrillary matrix with a capillary network, without necrosis. Lipidized cells resembling mature adipocytes, each with a single large vacuole that displaced the nucleus to the periphery, were scattered among the tumor cells (Fig. 1a, b). The tumor cells were diffusely positive for synaptophysin (Fig. 1c), many were positive for NeuN (Fig. 1d), and they were negative for GFAP and OLIG2. The MIB-1 labeling index was 1.9–2.1% (Table 1).

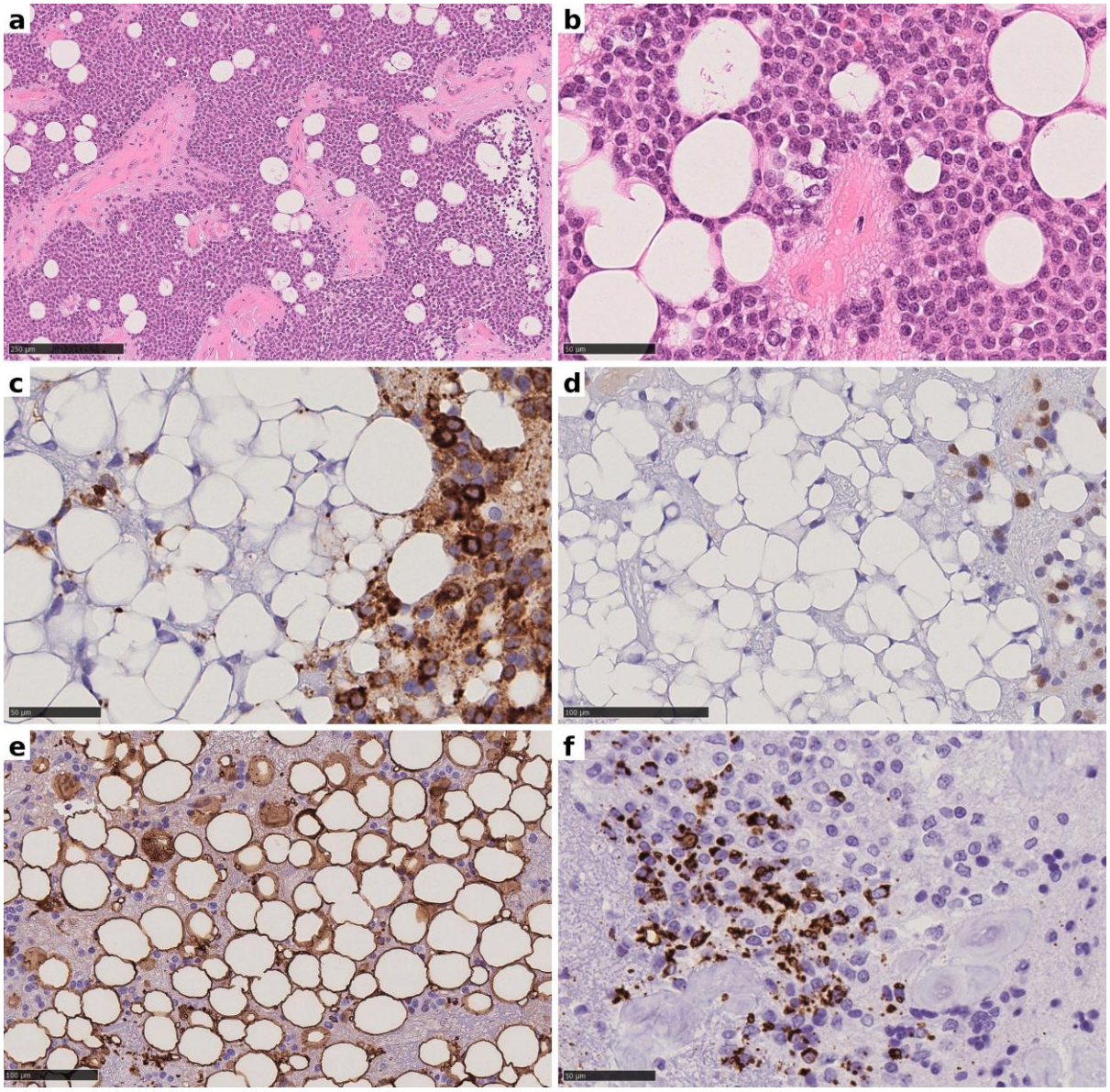

Fig. 1 Histological and immunohistochemical features. a, b Case 1, hematoxylin and eosin staining. a Tumor cells with relatively uniform round nuclei proliferate diffusely, with scattered lipidized cells and hyalinized vessels. b Lipidized cells contain a single large vacuole that displaces the nucleus to the periphery. c–e Case 2. c Synaptophysin is positive in the tumor cells (right) but lacks granular staining around the droplets of a cluster of lipidized cells (left). d NeuN is positive in the nuclei of tumor cells (right). e Perilipin-1 outlines the unilocular lipid droplets of lipidized cells. f Case 3. Small perilipin-1-positive droplets in tumor cells without a large vacuole. Scale bars: a 250 µm; b, c, f 50 µm; d, e 100 µm

Lipid droplets and lipidized cells

In all cases, perilipin-1 outlined the large lipid droplet of each lipidized cell (Fig. 1e) and labeled small droplets in some tumor cells without a large vacuole (Fig. 1f). Cases 2 and 3 also contained tumor cells with medium-sized droplets. Synaptophysin around the droplets was difficult to assess, but some lipidized cells lacked the granular staining seen around tumor cells (Fig. 1c).

DNA methylation-based classification

To determine the methylation classes of the cases, we applied the Heidelberg classifier and two crossNN models. All three arrays met the quality criteria. The Heidelberg classifier v12.8 classified all three cases as central neurocytoma at every hierarchical level from superfamily to subclass (calibrated scores 0.998, 0.990, and 0.999). Both crossNN models classified the cases as CN, with confidence scores of 0.72, 0.76, and 0.77 (Heidelberg-cohort model) and 0.57, 0.65, and 0.64 (pan-cancer model) (Fig. 2a and Table 1). All 90 CN from GSE288337 were classified as CN by both models (88 above the threshold with the pan-cancer model). Neither EVN was classified as CN.

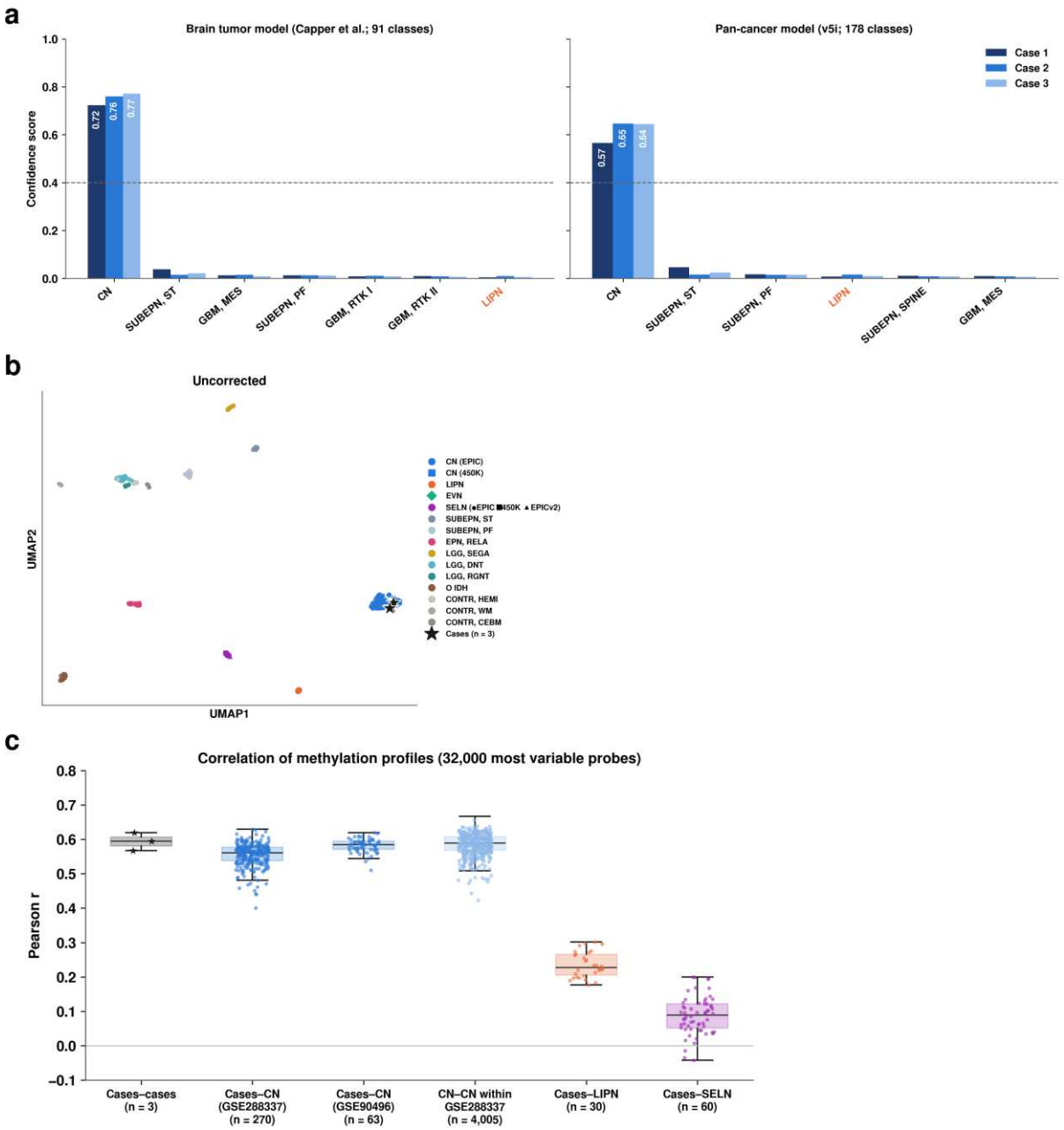

Fig. 2 DNA methylation-based classification and comparison with reference data. a Confidence scores of the three cases with the two crossNN models (left, Heidelberg-cohort model with 91 classes; right, pan-cancer model with 178 classes). The six classes with the highest mean scores and LIPN (orange) are shown, and the dashed line indicates the threshold (0.4). b UMAP of 345 samples based on the 10,000 most variable probes. Blue, CN (circles EPIC, squares 450K). Orange, LIPN. Green diamonds, EVN. Purple, SELN (circles EPIC, squares 450K, triangles EPICv2). Other colors, reference classes and non-neoplastic

controls. Black stars, the three cases. c Pearson correlations of methylation profiles (32,000 most variable probes) among the cases, between the cases and reference CN, LIPN, or SELN, and among CN from GSE288337. Boxes show the median and interquartile range (whiskers, 1.5 × interquartile range), and n indicates the number of sample pairs

We also used the model retrained with SELN, because neither published model contains a SELN class. In cross-validation, this model classified all 20 SELN as SELN. The final model classified the cases as CN (scores 0.59–0.66, SELN scores ≤ 0.016), whereas the models that were not retrained never classified SELN as CN (Online Resource 2, Supplementary Fig. 1).

Unsupervised comparison with reference data

To compare the cases with reference samples independently of classifier training, we performed UMAP and correlation analyses. All 345 samples met the quality criteria, and 217,776 probes without missing values across all samples were analyzed. In UMAP, the cases lay within the CN cluster, which comprised CN from both GSE288337 and GSE90496 and was separate from LIPN, EVN, and SELN (Fig. 2b). This held for all n_neighbors values and after FFPE correction. SELN formed a single cluster irrespective of array type.

Because UMAP is a visualization, we quantified similarity by correlation, using CN processed in a single batch as a reference (Fig. 2c). The correlation among the cases (median r = 0.594) was similar to the correlation between the cases and CN from GSE288337 (median 0.561), as well as the correlation between the cases and CN from GSE90496 (median 0.585). The correlation among the cases was also similar to the correlation among CN from GSE288337 (median 0.589). The cases correlated poorly with LIPN (median 0.227) and SELN (median 0.089).

Copy-number profiles

We examined copy-number changes characteristic of LIPN and EVN. The noise parameter of

the cases was 0.50–0.59. After exclusion of samples with a noise parameter > 0.6 (62 of the 90 CN from GSE288337 and 5 of the 20 SELN), the profiles of the cases were flat (Fig. 3a), as were those of the 28 remaining reference CN except one with a chromosome 5 gain. Neither chromosome 14 nor 2p loss was present in the cases (arm-level log2 ratios −0.011 to 0.019 and −0.006 to 0.006, respectively), whereas chromosome 14 loss was found in seven and 2p loss in three of the ten LIPN. A shallow chromosome 19 decrease in two cases was attributed to technical variation (Online Resource 1 and Online Resource 2, Supplementary Fig. 2). Profiles generated by the Heidelberg classifier showed no arm-level changes, focal amplifications, or homozygous deletions (Online Resource 2, Supplementary Fig. 3). The *FGFR1–TACC1* values of the cases (−0.135 to −0.081) lay within those of the 28 reference CN (−0.199 to −0.034), whereas the EVN that passed the noise criterion exceeded all CN (0.102). The other EVN was excluded (noise 0.606).

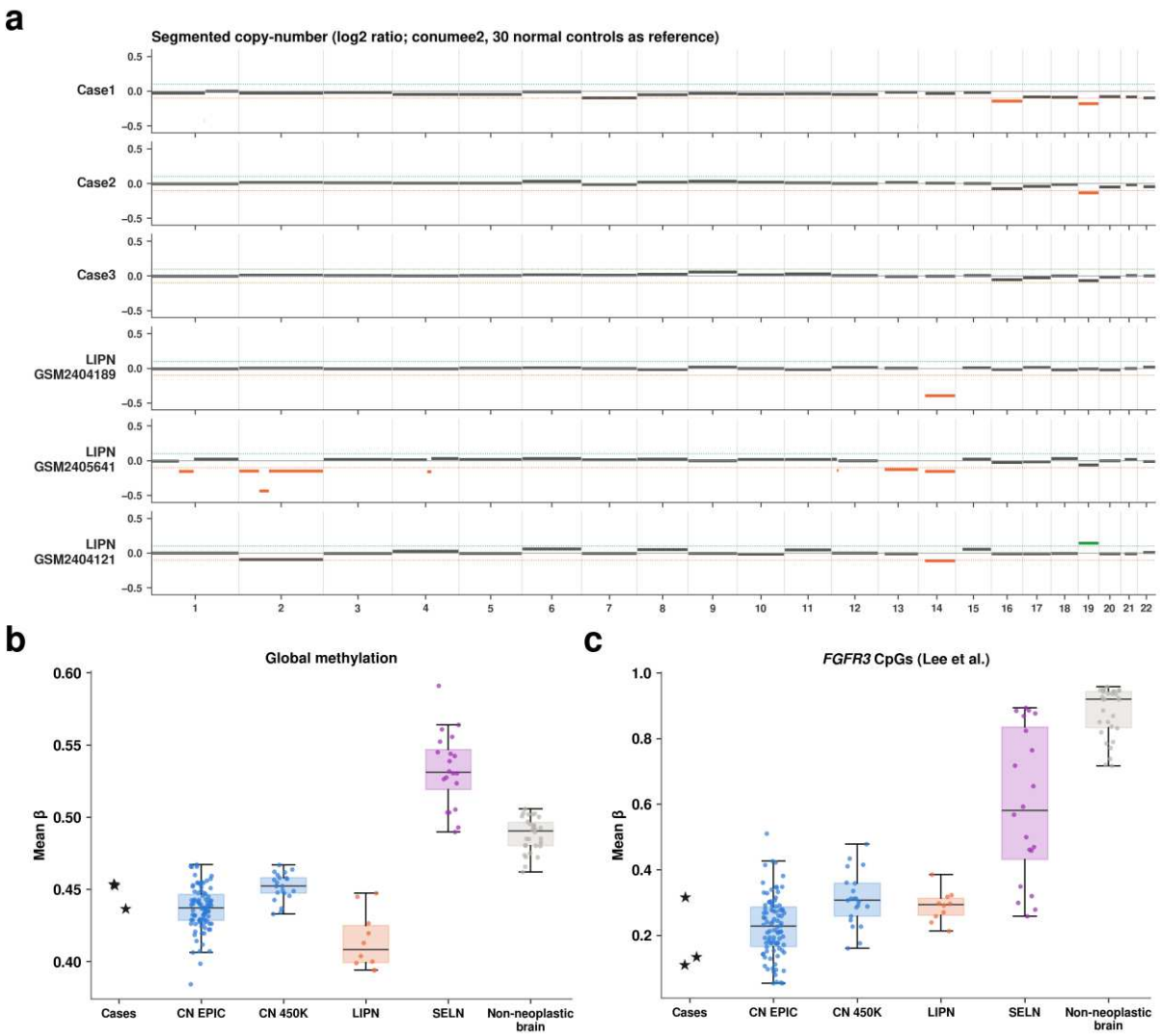

Fig. 3 Copy-number profiles and global and *FGFR3* methylation. a Copy-number profiles of the three cases and three representative LIPN with chromosome 14 loss (conumee2, with 30 non-neoplastic brain samples as reference). Segment mean log2 ratios below −0.1 are shown in orange and those above 0.1 in green. Dotted lines indicate ±0.1. b Global methylation (mean beta value after minfi noob preprocessing, excluding probes containing single-nucleotide polymorphisms and probes on the X and Y chromosomes). c Mean beta value of the three *FGFR3* CpGs reported by Lee et al. In b and c, stars indicate the cases, and boxes show the median and interquartile range (whiskers, 1.5 × interquartile range) of CN profiled on EPIC (n = 90) and 450K (n = 21), LIPN (n = 10), SELN (n = 20), and non-neoplastic brain (n = 30)

Global and FGFR3 methylation

Because global and *FGFR3* hypomethylation have been reported as features of CN [15, 16], we examined both in the cases. Global methylation was lower in reference CN (mean 0.440, n = 111) than in non-neoplastic brain samples (mean 0.488, n = 30, $P = 3.2 \times 10^{-26}$). The values of the cases (0.453, 0.453, and 0.436) were within the range of reference CN and below those of all non-neoplastic samples, whereas LIPN had a median of 0.408 (Fig. 3b). The mean beta value of the three *FGFR3* CpGs in the cases (0.11, 0.32, and 0.13) was comparable to that of reference CN (median 0.23 for EPIC and 0.31 for 450K) and far below that of non-neoplastic samples (median 0.92) (Fig. 3c). LIPN also showed *FGFR3* hypomethylation (median 0.29).

LIPN-associated methylation differences in the cases

To test whether the cases share the methylation differences of LIPN, including those at adipogenesis-related genes [20], we compared CN and LIPN of the reference cohort. In this cohort, 42,976 CpGs and 6,253 DMRs (5,057 hypomethylated and 1,196 hypermethylated in LIPN) differed between CN and LIPN, and the direction of the difference was reproduced in 95.3% of DMRs in GSE109379 (r = 0.89). DMRs at *NFATC1*, *ZFPM1*, *PLIN4*, *PNPLA2*, *ADIPOQ*, and *LIPE* were hypomethylated and those at *DLK1* hypermethylated in LIPN. The cases had LIPN scores (−0.44, −0.37, and −0.42) within the range of reference CN (−0.45 to −0.29) and far from LIPN (+0.18 to +0.30), and their methylation at each of these genes was within or near the range of reference CN (Fig. 4). SELN were intermediate (median −0.05, Online Resource 1).

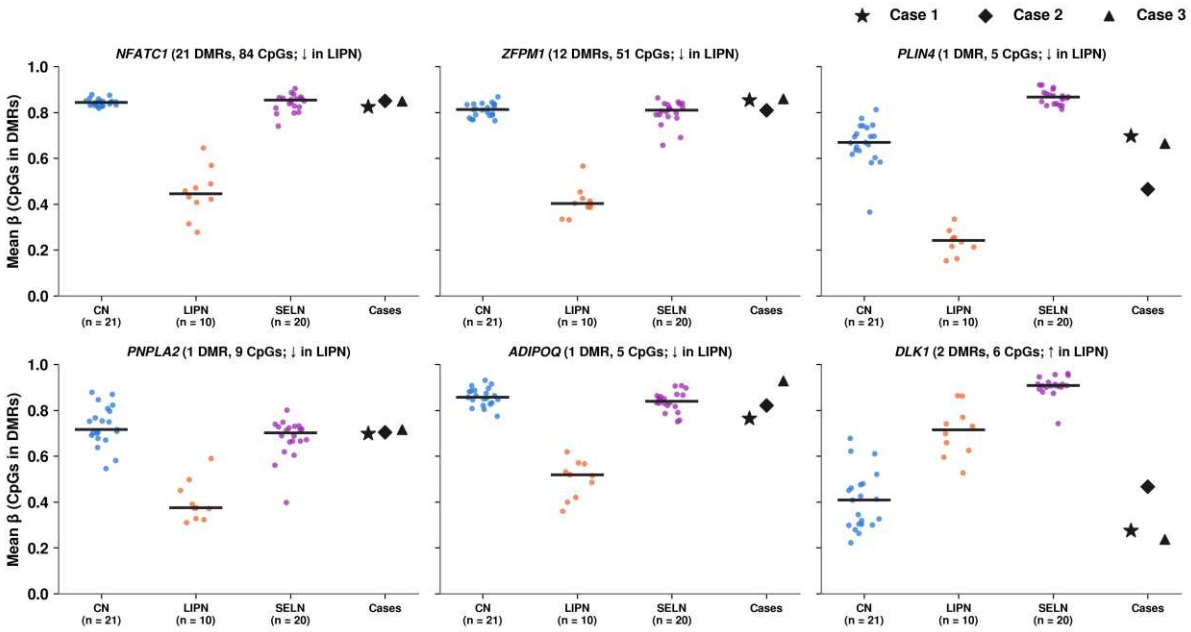

Fig. 4 Methylation of adipogenesis-related genes at CN–LIPN DMRs in reference neurocytomas and the cases. For each gene, the mean beta value of all CpGs within its DMR(s) is shown for CN (n = 21) and LIPN (n = 10) of the reference cohort, SELN (n = 20, GSE331022), and the three cases. For *NFATC1*, *ZFPM1*, and *DLK1*, CpGs of multiple DMRs were averaged. *LIPE*, with a single DMR, is not shown. Horizontal bars indicate medians. ↓ and ↑ indicate hypomethylation and hypermethylation in LIPN, respectively

Discussion

For lateral ventricular neurocytomas with lipidized cells, DNA methylation profiling could show one of five outcomes. They could (i) belong to CN, (ii) belong to LIPN, (iii) belong to another group such as SELN, (iv) form a distinct methylation class, or (v) match no class consistently, as EVN initially did [7].

Our data support the first possibility, that these tumors belong to CN. All three cases were classified as CN by the Heidelberg classifier and both crossNN models with scores in the range of independent reference CN. They lacked the chromosome 14 and 2p losses frequent in LIPN. Unlike the EVN controls, which form a distinct class, the cases were classified as

CN and lay within the CN cluster in unsupervised analysis. Global and *FGFR3* hypomethylation were consistent with the reported features of CN [15, 16], although *FGFR3* hypomethylation was also found in LIPN and does not discriminate the two on its own. The cases were also distinct from SELN in both the SELN-augmented classifier and the unsupervised analysis. These findings support classifying lateral ventricular neurocytomas with lipidized cells as CN, rather than as an intraventricular counterpart of LIPN or a separate entity such as the proposed central liponeurocytoma [30].

Lipomatous change is described as an occasional finding in CN [29]. George and Scheithauer regarded a lateral ventricular case as tumoral lipidization of a neurocytoma [11], whereas Xu et al. noted that intraventricular liponeurocytomas differ from LIPN in sex and age distribution [30]. Zanoni et al. emphasized that fat alone does not confirm liponeurocytoma [32]. Our data thus show that lipidized cells are not specific to LIPN, and a diagnosis of LIPN should not rest on lipidized cells alone.

Our comparison of public CN and LIPN reference datasets detected methylation differences at adipogenesis-related genes reported in LIPN [20], including hypermethylation of the preadipocyte factor *DLK1* [28]. Our cases were within or near the range of reference CN at all of these genes. Thus, the bulk methylation profiles of the cases provide no evidence of the adipogenic methylation changes seen in LIPN, although changes confined to the minority of lipidized cells cannot be excluded.

Lipidized cells have been interpreted as lipidized neurocytic cells, with small droplets coalescing into large ones [11, 14], as true adipose metaplasia [12], or as cells derived from pluripotent progenitors [23]. Perilipin-1 identified small droplets in tumor cells without a large vacuole and medium-sized droplets in Cases 2 and 3, consistent with intracellular lipid accumulation and droplet coalescence [11, 14]. Because perilipin-1 also coats lipid droplets in non-adipocytes [25], these findings identify lipid droplets but do not indicate adipocytic

differentiation. Some lipidized cells lacked synaptophysin around the droplet, suggesting that at least some may have lost neuronal features, whereas lipidized cells in LIPN have mostly been reported to retain neuronal markers [2, 5].

This study has limitations. First, it included only three cases, all profiled on the EPICv2 array in a single laboratory, without reference CN profiled on this platform. The similarity among the cases cannot be separated from platform or batch effects, and whether CN with lipidized cells form a subgroup within CN remains open. Second, in the copy-number analysis, 62 of the 90 EPIC-profiled FFPE CN exceeded the noise threshold. Third, the SELN-augmented classifier was trained on only 20 SELN from a single study. Fourth, the comparison of CN and LIPN relied on ten LIPN from a single cohort and one independent LIPN. Patient age, which is higher in LIPN than in CN [29], was unavailable and could not be adjusted for. CN-like methylation in the cases does not exclude adipogenic changes in lipidized cells, because bulk profiling cannot resolve changes confined to a minority of cells. Fifth, the immunohistochemical evaluation was qualitative, and the markers were not examined in the same cells or on serial sections.

In conclusion, DNA methylation and copy-number profiling indicate that lateral ventricular neurocytomas with lipidized cells belong to CN. Lipidized cells are therefore not specific to LIPN and can occur within the morphological spectrum of CN.

Acknowledgments

We thank Hiromi Mohri, Miho Kimura, and Kozue Mori for assistance with specimen preparation, antibody optimization, and immunostaining, and Nanami Okugawa for English proofreading. This study was conducted on the Platform for Research Innovation and Support in Medicine – Hokkaido University (PRISM–HU).

Declarations

Author contributions Y.O., Z.T., Sa.T., Y.M., K.I., Y.S., M.K., H.S., L.W., and M.T. contributed to the pathological diagnosis. Y.F., H.M., Y.I., S.Y., and M.F. performed the surgery. K.S. and J.S. generated the DNA methylation data. T.K. and T.Y. analyzed the data. Sh.T. supervised the study. T.K. wrote the first draft of the manuscript, and all authors read and approved the final manuscript.

Funding This work was supported by the Japan Society for the Promotion of Science (JSPS) KAKENHI Scientific Research S (24H00037:ST). This research was supported by the Japan Agency for Medical Research and Development (AMED) under Grant Number JP256f0137006.

Conflict of interest The authors declare that they have no conflict of interest.

Ethics approval This study was approved by the Ethical Review Board for Life Science and Medical Research, Hokkaido University Hospital (approval number 025-0260) and was performed in accordance with the Declaration of Helsinki.

Consent to participate An opt-out procedure was implemented.

Data availability The IDAT files of the three cases are available from the corresponding author upon reasonable request. The public datasets analyzed in this study are available from the Gene Expression Omnibus under accession numbers GSE90496, GSE109379, GSE152653, GSE288337, and GSE331022. The analysis code is available at https://github.com/chykuwa-ctrl/CN_lipidized_methylation and archived at Zenodo (https://doi.org/10.5281/zenodo.23937641).

References

1. Al-Umran MR, Al-Umran SR, Arab AF et al (2021) Lateral ventricular liponeurocytoma: review of literature and case illustration. Neurochirurgie 67:579–586

2. Anghileri E, Eoli M, Paterra R et al (2012) FABP4 is a candidate marker of cerebellar liponeurocytomas. J Neurooncol 108:513–519

3. Aryee MJ, Jaffe AE, Corrada-Bravo H et al (2014) Minfi: a flexible and comprehensive Bioconductor package for the analysis of Infinium DNA methylation microarrays. Bioinformatics 30:1363–1369

4. Bankhead P, Loughrey MB, Fernández JA et al (2017) QuPath: open source software for digital pathology image analysis. Sci Rep 7:16878

5. Buccoliero AM, Caldarella A, Bacci S et al (2005) Cerebellar liponeurocytoma: morphological, immunohistochemical, and ultrastructural study of a relapsed case. Neuropathology 25:77–83

6. Capper D, Jones DTW, Sill M et al (2018) DNA methylation-based classification of central nervous system tumours. Nature 555:469–474

7. Capper D, Stichel D, Sahm F et al (2018) Practical implementation of DNA methylation and copy-number-based CNS tumor diagnostics: the Heidelberg experience. Acta Neuropathol 136:181–210

8. Daenekas B, Pérez E, Boniolo F et al (2024) Conumee 2.0: enhanced copy-number variation analysis from DNA methylation arrays for humans and mice. Bioinformatics 40:btae029

9. Eckhardt A, Drexler R, Schoof M et al (2024) Mean global DNA methylation serves as independent prognostic marker in IDH-wildtype glioblastoma. Neuro Oncol 26:503–513

10. Gembruch O, Junker A, Mönninghoff C et al (2018) Liponeurocytoma: systematic review of a rare entity. World Neurosurg 120:214–233

11. George DH, Scheithauer BW (2001) Central liponeurocytoma. Am J Surg Pathol 25:1551–1555

12. Gupta K, Salunke P, Kalra I, Vasishta RK (2011) Central liponeurocytoma: case report and review of literature. Clin Neuropathol 30:80–85

13. Horoupian DS, Shuster DL, Kaarsoo-Herrick M, Shuer LM (1997) Central neurocytoma:

one associated with a fourth ventricular PNET/medulloblastoma and the second mixed with adipose tissue. Hum Pathol 28:1111–1114

14. Jackson TR, Regine WF, Wilson D, Davis DG (2001) Cerebellar liponeurocytoma. Case report and review of the literature. J Neurosurg 95:700–703

15. Krech M, Muench A, Teichmann D et al (2025) Outcome-associated factors in a molecularly defined cohort of central neurocytoma. Acta Neuropathol 149:61

16. Lee Y, Chowdhury T, Kim S et al (2024) Central neurocytoma exhibits radial glial cell signatures with FGFR3 hypomethylation and overexpression. Exp Mol Med 56:975–986

17. Lucas CG, Gupta R, Doo P et al (2020) Comprehensive analysis of diverse low-grade neuroepithelial tumors with FGFR1 alterations reveals a distinct molecular signature of rosette-forming glioneuronal tumor. Acta Neuropathol Commun 8:151

18. Maksimovic J, Oshlack A, Phipson B (2021) Gene set enrichment analysis for genome-wide DNA methylation data. Genome Biol 22:173

19. McInnes L, Healy J, Melville J (2018) UMAP: uniform manifold approximation and projection for dimension reduction. arXiv:1802.03426. https://doi.org/10.48550/arXiv.1802.03426

20. Pearce TM, Cimino PJ, Lucas CG et al (2026) Sellar region neurocytomas exhibit a CIMP and neuroendocrine-like epigenetic signature distinct from other intra-axial neurocytomas. Acta Neuropathol 152:20

21. Peters TJ, Buckley MJ, Statham AL et al (2015) De novo identification of differentially methylated regions in the human genome. Epigenetics Chromatin 8:6

22. Peters TJ, Meyer B, Ryan L et al (2024) Characterisation and reproducibility of the HumanMethylationEPIC v2.0 BeadChip for DNA methylation profiling. BMC Genomics 25:251

23. Rajesh LS, Vasishta RK, Chhabra R, Banerjee AK (2003) Case report: central liponeurocytoma. Neuropathol Appl Neurobiol 29:511–513

24. Ritchie ME, Phipson B, Wu D et al (2015) limma powers differential expression analyses for RNA-sequencing and microarray studies. Nucleic Acids Res 43:e47

25. Sánchez-Romero C, Carreón-Burciaga R, Gónzalez-Gónzalez R et al (2021) Perilipin 1 and adipophilin immunoexpression suggests the presence of lipid droplets in tooth germ, ameloblastoma, and ameloblastic carcinoma. J Oral Pathol Med 50:708–715

26. Sievers P, Stichel D, Schrimpf D et al (2018) FGFR1:TACC1 fusion is a frequent event in molecularly defined extraventricular neurocytoma. Acta Neuropathol 136:293–302

27. Sill M, Schrimpf D, Patel A et al (2026) Advancing CNS tumor diagnostics with expanded DNA methylation-based classification. Cancer Cell 44:340–354

28. Smas CM, Sul HS (1993) Pref-1, a protein containing EGF-like repeats, inhibits adipocyte differentiation. Cell 73:725–734

29. WHO Classification of Tumours Editorial Board (2021) Central nervous system tumours. WHO classification of tumours series, 5th edn, vol 6. International Agency for Research on Cancer, Lyon

30. Xu L, Du J, Wang J et al (2017) The clinicopathological features of liponeurocytoma. Brain Tumor Pathol 34:28–35

31. Yuan D, Jugas R, Pokorna P et al (2025) crossNN is an explainable framework for cross-platform DNA methylation-based classification of tumors. Nat Cancer 6:1283–1294

32. Zanoni DK, Abath Neto OL, Shekhrajka N et al (2025) Lateral ventricle central neurocytoma with lipidization: a case report of an underrecognized presentation. Arq Neuropsiquiatr 83:s00451806925

33. Zhou W, Triche TJ Jr, Laird PW, Shen H (2018) SeSAMe: reducing artifactual detection of DNA methylation by Infinium BeadChips in genomic deletions. Nucleic Acids Res 46:e123

Electronic supplementary material

Online Resource 1 Supplementary methods and results: antibodies for immunohistochemistry, crossNN preprocessing and retraining, reference set and sample filtering for the unsupervised analysis, copy-number analysis, and the comparison of CN and LIPN (PDF)

Online Resource 2 Supplementary Figs. 1–3 (PDF). Supplementary Fig. 1 crossNN classification including sellar region neurocytoma (SELN). Supplementary Fig. 2 Chromosome 19 log2 ratio versus the mean log2 ratio of the GC-rich arms 17q and 22q. Supplementary Fig. 3 Genome-wide copy-number profiles of the three cases generated by the

444 Heidelberg classifier v12.8

445

Supplementary Files

This is a list of supplementary files associated with this preprint. Click to download.

- ESM1.pdf
- ESM2.pdf